American Journal of Pathology, Vol. 149, No. 2, August 1996

Short Communication

Chronic Iron Overload in Rats Induces Oval Cells in the Liver

Patrick G. J. Smith and George C. T. Yeoh

From the Department of Biochemistry, University of Western Australia, Nedlands, Australia

Liver damage induced by a variety of agents including hepatocarcinogens, alcohol, and virus induces proliferation of oval cells. In this study, iron overloading of the liver is used as a means of inducing liver damage over an extended period to ascertain whether it promotes the appearance of oval cells. Rats were fed a 2% carbonyl-iron-supplemented diet for 3 or 6 months. Extensive iron deposits appeared periportally in hepatocytes and some Kupffer cells. Iron deposition was less pronounced pericentrally. Small oval-like cells, morphologically and immunocytochemically similar to CDE-derived oval cells, were identified and quantified. They first emerged periportally and subsequently in small tracts or foci nearer central regions and stained positively for α-fetoprotein, π-class glutathione S-transferase, and the embryonic form of pyruvate kinase. They contained very few iron deposits and were classified as iron free. The major difference between CDE- and iron-overload-derived oval cells was that the latter were negative for transferrin. This study shows that cellular changes occurring in iron-overloaded rat liver are similar to those observed in rats placed on a hepatocarcinogenic diet and in rats chronically exposed to alcohol. (Am J Pathol 1996, 149:389–398)

The emergence of oval cells in preneoplastic liver during experimentally induced hepatocarcinogenesis is well documented.[1–9] These cells were characterized in 1956[2] and described as small cells having scanty, lightly basophilic cytoplasm and ovoid nuclei. They have been shown to express embryonic proteins, for example, α-fetoprotein (AFP),[10] as well as embryonic enzymes such as the M_2 form of pyruvate kinase (M_2-PK)[3] and π-class glutathione S-transferase (π-GST).[11] During experimental hepatocarcinogenesis, oval cells are initially located periportally and subsequently spread throughout the liver lobule. The ability of these cells to give rise to hepatomas has been demonstrated.[8]

More recently, oval cells have been described in other conditions such as hepatitis[12] and alcohol-induced liver toxicity.[13] A common factor in these conditions is prolonged liver damage.

Genetic hemochromatosis (GH) is an autosomal recessive disorder with the abnormal gene located on the short arm of the sixth chromosome near the A locus of the histocompatibility leukocyte antigens system.[14–17] Among people of Northern European descent, GH is a common cause of iron overload with approximately 1 in 220 people being affected.[14] Major complications of GH are cirrhosis of the liver,[15,18–26] congestive heart failure,[25–28] and diabetes.[26,27] In particular, the disease has been associated with a substantially increased risk of developing primary hepatocellular carcinoma.[18,20,21,24–26,29,30]

The basis of cellular and tissue injury caused by chronic parenchymal iron overload is still unclear.[15] There is agreement that cell toxicity is associated with iron-induced lipid peroxidation and the associated organelle dysfunction mediated by production of free radicals.[15,16,19,23,31–33] Factors such as alcoholism and hepatitis B virus infection have also been implicated in the pathogenesis of GH.[34–41]

Supported by grant number 92/0063 from the National Health and Medical Research Council of Australia and funding from the Faculty of Medicine, University of Western Australia.

Accepted for publication April 12, 1996.

Address reprint requests to Dr. George C. T. Yeoh, Department of Biochemistry, University of Western Australia, Nedlands, Western Australia, Australia 6907.

Despite strong clinical evidence supporting the relationship between chronic iron overload and the development of hepatocellular carcinoma, the specific mechanisms leading to hepatoma formation in iron overload are unknown. It has been suggested that increased free radical production is responsible for heritable genetic alterations that increase the likelihood of transformation to cancer.[26] An alternative explanation proposes that cellular changes that accompany iron-induced liver damage are similar to those observed when liver cancer is induced by carcinogens. Specifically, these conditions promote the proliferation of oval cells. The present study documents the induction of oval cells in liver subjected to iron overload toxicity.

Materials and Methods

Animals

Males of the Wistar strain of the albino rat *Rattus norvegicus* (120 to 140 g) were used in these experiments and received humane care in compliance with guidelines set out by the National Health and Medical Research Council of Australia.

Iron Overload Diet

Rats were fed a carbonyl-iron-supplemented diet and normal drinking water for 3 to 6 months. Ferronyl (ISP Australasia, Sydney, Australia) was blended with a standard laboratory chow to a final concentration of 2% (w/w). Control rats received a standard laboratory chow.

Choline-Deficient, Ethionine-Supplemented (CDE) Diet

Rats were fed a choline-deficient diet (product code TD 79246, Teklad, Madison, WI) plus 0.15% (w/v) DL-ethionine supplemented in their drinking water (CDE group) for 3 weeks. Based on their consumption of liquid, this was equivalent to giving the rats a 0.07% (w/v) ethionine-supplemented diet in solid form. Ethionine given in the drinking water minimized our risk of exposure to the carcinogen. Control rats received a standard laboratory chow.

Elutriation of Liver Cells

The liver of control and iron-overloaded rats were perfused via the hepatic portal vein with perfusion buffer (0.4 mg/ml KCl, 6.8 mg/ml NaCl, 4.8 mg/ml HEPES, 2.1 mg/ml $NaHCO_3$, 1.0 mg/ml glucose, pH 7.4, 300 mOsmol/L) under surgical anesthesia (1 μl/g body weight Nembutal; Pentobarbitone sodium (60 mg/ml) Boehringer Ingelheim, Artarmon, NSW, Australia). Liver cells were isolated by collagenase perfusion using the method of Seglen[42] and separated according to size and density by centrifugal elutriation as described by Yaswen et al.[10] Four fractions were collected at flow rates of 18, 24, 40, and 50 ml/minute, and a fifth fraction was obtained by shutting down the rotor (from 2500 rpm) while the flow rate was maintained at 50 ml/minute. A preelutriation sample was also retained for analysis. When present, some oval cells were collected in fraction 4, although the majority were contained in fraction 3, which was free of adult hepatocytes as determined by routine histochemistry and immunocytochemical staining. Fractions were attached to poly-L-lysine-coated glass slides by cytocentrifugation and fixed in 4% paraformaldehyde, 0.1% glutaraldehyde in 0.1 mol/L sodium cacodylate buffer (pH 7.45) for 4 minutes at 4°C.

Histochemistry and Immunocytochemistry

Before digestion with collagenase, samples of liver were removed and cut into approximately 0.5-cm^3 pieces and immersed in Carnoy's fixative for 6 hours and then embedded in paraffin wax. For light microscopy, 6-μm sections were cut and attached to glass slides coated with poly-L-lysine. Liver sections and cytocentrifuged cell preparations were stained with haematoxylin and chromotrope 2R (H&C) to verify morphology. Liver sections were also stained for hemosiderin using Perls' Prussian blue method (1% potassium ferrocyanide in 1% HCl) to confirm the status of iron overload. Kupffer cells were identified by staining for endogenous peroxidase by treatment with 0.05% diaminobenzidine color reagent and 0.01% H_2O_2 in 0.05 mol/L Tris, pH 7.45, for 20 minutes. Immunocytochemistry was performed at room temperature using the indirect immunoperoxidase method. Specific antibodies used were those raised against the M_2 isoenzyme of pyruvate kinase (M_2-PK), a fetal isoenzyme; the L form of pyruvate kinase (L-PK), the adult specific isoenzyme; AFP; α-, μ-, and π-GST; tyrosine aminotransferase (TAT); transferrin (TF); and albumin (ALB). Samples treated with nonimmune serum were incorporated as negative controls. Before immunocytochemistry, endogenous peroxidase activity was blocked by treating with 2.5% aqueous periodic acid for 5 minutes and 0.02% sodium borohydride for 2 minutes.[30] This was followed by a 1-hour incubation in 10% fetal calf serum

and 0.2% saponin in phosphate-buffered saline (PBS). Samples were then reacted for 1 hour with the following primary antibodies: L-PK, α-, μ-, and π-GST, TF, and ALB (1:200 dilution); M_2-PK (1:500 dilution); AFP (1:400 dilution); TAT or nonimmune serum (1:100 dilution). After three washes with 0.2% saponin-PBS, the samples were exposed to a 1:200 dilution of the secondary antibody (horseradish-peroxidase-conjugated goat IgG directed against rabbit IgG (H+L) from Diagnostics Pasteur, Marnes-la-Coquette, France) for 1 hour. The washing procedure was repeated followed by a rinse in 0.05 mol/L Tris, pH 7.45. The secondary antibody was visualized by reaction with 0.05% diaminobenzidine and 0.01% H_2O_2 in 0.05 mol/L Tris, pH 7.45, for 20 minutes. The samples were then washed with PBS and mounted with Kaiser's glycerol gelatin (Merck, Darmstadt, Germany).

Cell Counts

Liver sections stained for M_2-PK were used to determine the proportion of oval cells present in the liver at each time point. Using a standard graticule, several fields of view were counted. Cells were scored when they satisfied the morphological criteria of oval cells and expressed M_2-PK. Hepatocytes in the same field of view were also scored, and the results are expressed as the number of M_2-PK-positive oval cells per 100 hepatocytes. To determine the proportion of oval cells that expressed a particular marker, cytocentrifuged preparations from fraction 3, which is highly enriched for oval cells, were scored. Positive oval cells were expressed as a percentage of total cells.

Results

In Vivo *Histological and Immunocytochemical Changes in the Liver*

CDE-Treated Rats

Oval cell proliferation resulted in extensive alteration of the hepatic architecture. Tracts of oval cells (Figure 1a, small arrows) were evident throughout the liver lobule between clusters of hepatocytes (Figure 1a, large arrows). In histological preparations, oval cells were identified by size (approximately one-third to one-quarter of a hepatocyte), a high nucleus-to-cytoplasm ratio, possession of an ovoid nucleus, and weakly basophilic cytoplasm. Immunologically, they expressed the embryonic isoenzymes of pyruvate kinase (M_2-PK, Figure 1b, small arrows) and glutathione S-transferase (π-GST; data not shown) as well as AFP (data not shown). Hepatocytes did not express M_2-PK (Figure 1b, large arrow), although a minority expressed both π-GST and AFP (data not shown). More than 95% of CDE-derived oval cells were positive for M_2-PK and π-GST, with just over one-third positive for AFP. A minority expressed the adult liver enzymes α-GST, μ-GST, and TAT. Approximately one-third expressed the parenchymal cell markers TF and ALB. Control rats showed no evidence of oval cell proliferation.

Iron-Overloaded Rats

Before *in situ* perfusion, iron-loaded livers usually had a dark red/brown discoloration that persisted after perfusion. Control livers displayed the normal pale yellow appearance after perfusion.

In both 3- and 6-month iron-loaded liver samples there was a zonal distribution of iron deposition with a decrease toward pericentral regions, as shown by Perls' Prussian blue staining (Figure 1c, arrow). Extensive iron deposition was detected in all hepatocytes located periportally (Figure 1d, small arrow) as well as in a small proportion of Kupffer cells (Figure 1d, intermediate arrow). Kupffer cells were identified on serial sections by morphology and expression of endogenous peroxidase. Hepatocytes located pericentrally, although exhibiting weaker staining, were still iron loaded to varying degrees. Iron deposits were also visible without the aid of Prussian blue staining and appeared as yellow/brown granular deposits within the cytoplasm. Putative oval cells (Figure 1d, large arrow), as well as bile duct cells and endothelial cells, were relatively free of iron.

It is interesting to note that there was a zonal pattern of TF distribution that was inverse to the pattern of iron deposition. TF expression was maximal pericentrally (Figure 1e, small arrow) and decreased toward periportal regions (Figure 1e, large arrow) where iron deposition was maximal.

Small basophilic cells with oval cell morphology were detected around the portal regions of the 3-month iron-loaded liver samples (Figure 2a, small arrows). Large hepatocytes (Figure 2a, large arrow) were easily distinguished from the oval cells. The majority of these putative oval cells were positive for M_2-PK (Figure 2b, small arrows) whereas hepatocytes were negative (Figure 2b, large arrow). Putative oval cells were also positive for π-GST, with the majority exhibiting nuclear staining (Figure 2c, small arrows). A small proportion of hepatocytes were also π-GST positive, with evidence of nuclear staining (Figure 2c, large arrow). The oval cells were hetero-

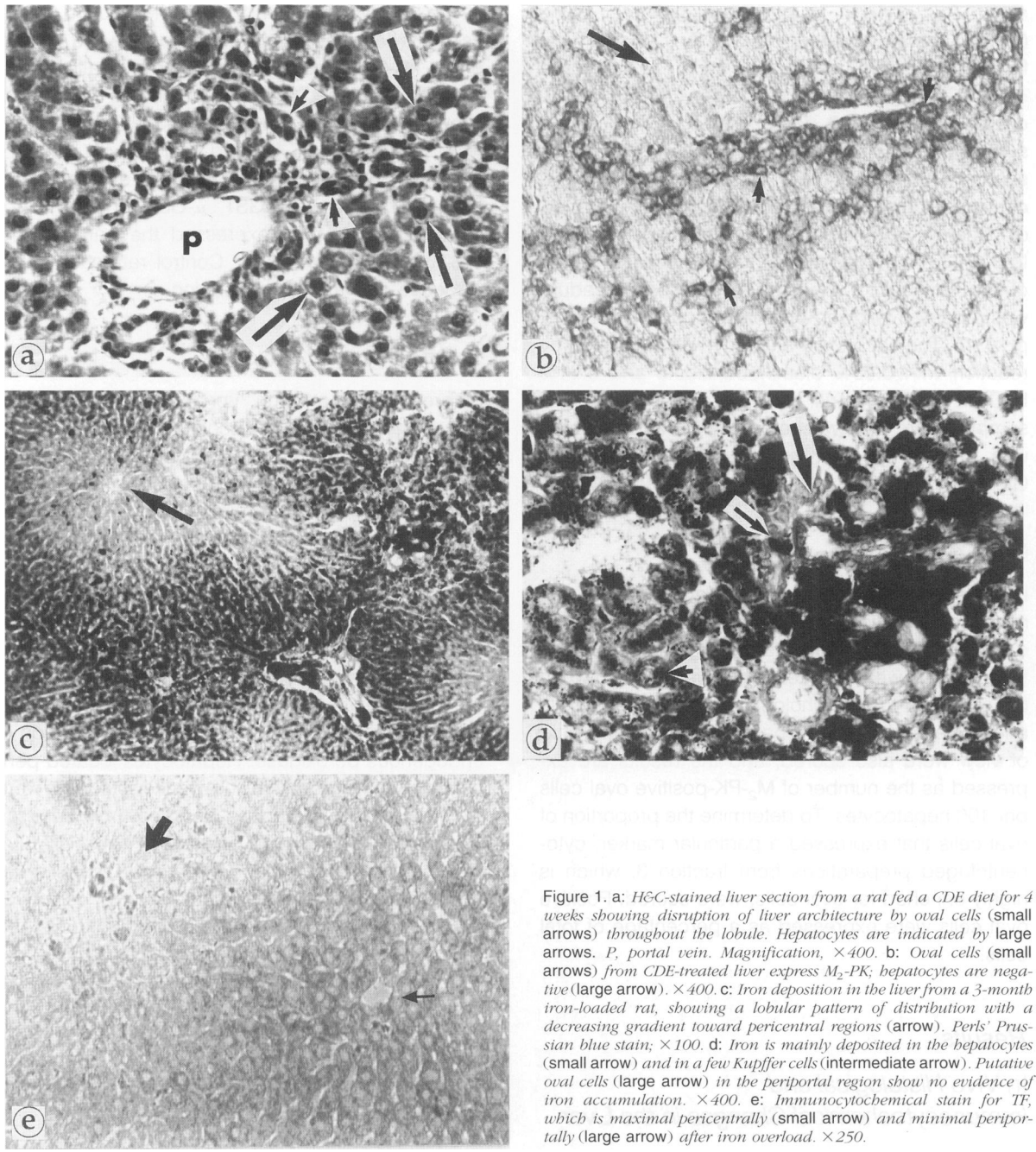

Figure 1. a: *H&E-stained liver section from a rat fed a CDE diet for 4 weeks showing disruption of liver architecture by oval cells* (small arrows) *throughout the lobule. Hepatocytes are indicated by* large arrows. *P, portal vein. Magnification, ×400.* b: *Oval cells* (small arrows) *from CDE-treated liver express M_2-PK; hepatocytes are negative* (large arrow). *×400.* c: *Iron deposition in the liver from a 3-month iron-loaded rat, showing a lobular pattern of distribution with a decreasing gradient toward pericentral regions* (arrow). *Perls' Prussian blue stain; ×100.* d: *Iron is mainly deposited in the hepatocytes* (small arrow) *and in a few Kupffer cells* (intermediate arrow). *Putative oval cells* (large arrow) *in the periportal region show no evidence of iron accumulation. ×400.* e: *Immunocytochemical stain for TF, which is maximal pericentrally* (small arrow) *and minimal periportally* (large arrow) *after iron overload. ×250.*

geneous with respect to AFP expression, approximately one-quarter being positive (Figure 2d, small arrows). Fine granular iron deposits were visible in hepatocytes (Figure 2d, intermediate arrow) as were the larger and more dense iron deposits (Figure 2d, large arrow).

Oval cells also displayed a heterogeneous expression of hepatocytic markers such as ALB, L-PK, α-GST, μ-GST, and TAT. A minority expressed L-PK, α-GST, μ-GST, and TAT (Table 1) whereas approximately one-third expressed ALB (Table 1). The level of L-PK expression in the iron-loaded liver was diminished compared with control liver, and there was heterogeneity among hepatocytes (Table 1); however, there was no obvious zonal distribution of L-PK expression. A similar reduction in L-PK expression was also observed in the CDE-treated liver. Oval cells from iron-loaded liver were negative for TF.

Similar oval cells were found in the 6-month samples and with greater frequency. There were 10 ± 2.3 (mean ± SE) M_2-PK-positive oval cells per 100 hepatocytes in the liver after 3 months of iron load-

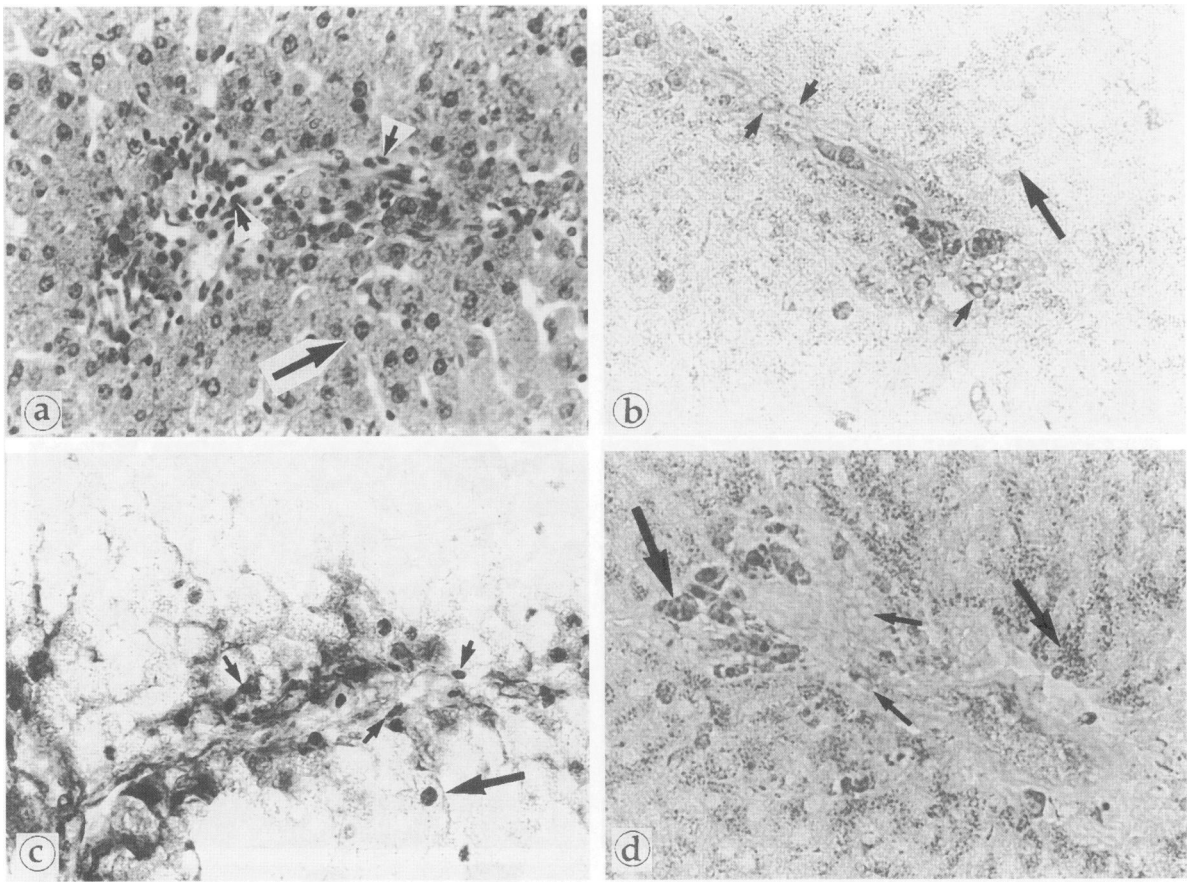

Figure 2. a: *H&C-stained liver section from a 3-month iron-loaded rat showing tracts of oval cells* (small arrows) *extending from a small portal region, surrounded by hepatocytes* (large arrow). *Magnification, ×400.* b: *M_2-PK-positive oval cells extending into the liver lobule* (small arrows). *Hepatocytes are negative* (large arrow). *×400.* c: *The majority of oval cells are π-GST positive and exhibit nuclear staining* (small arrows). *A small proportion of hepatocytes express π-GST with nuclear staining* (large arrow). *×400.* d: *Some oval cells express AFP* (small arrows). *Note the presence of granular iron deposits* (intermediate arrow) *as well as dense iron deposits* (large arrow). *×400.*

ing; which increased to 17 ± 3.1 (mean ± SE) after 6 months of iron loading. In addition to the increased quantity of oval cells in the 6-month samples, a significant proportion were pericentrally located, some of which formed small foci (Figure 3, a–d). These contained approximately 15 to 20 oval cells that were positive for M_2-PK (Figure 3a) and π-GST (data not shown). Hepatocytes were M_2-PK negative. The pattern of immunostaining for AFP, ALB, L-PK, and TAT were similar for the 6-month and 3-month samples. AFP expression, detected in only a few of the parenchymal cells at 3 months increased to approximately one-third by 6 months. Oval cells remained TF negative after 6 months of iron overload (Figure 3b, small arrow), giving the appearance of a TF-free focus surrounded by darkly stained parenchyma (Figure 3b, large arrow). The majority of oval cells were negative for α-GST, with only a few being weakly positive (Figure 3c, small arrow). The same was observed for μ-GST (Figure 3d, small arrow). All hepatocytes expressed both α-GST (Figure 3c, intermediate arrow) and μ-GST (Figure 3d, intermediate arrow). For both α- and μ-GST, hepatocytes exhibited either cytoplasmic staining and nuclear staining or cytoplasmic staining alone.

Ductal structures were observed in 5% of oval cell foci. In contrast to the surrounding oval cells, the ductal structures were strongly positive for μ-GST

Table 1. *Percentage of Isolated Oval Cells Expressing the Listed Markers after 4 Weeks of CDE Treatment or 3 to 6 Months of Iron Overloading*

Condition	AFP	ALB	TF	L-PK	M_2-PK	α-GST	μ-GST	π-GST	TAT
CDE (4 weeks)	39	53	47	19	95	13	27	95	10
Iron overload (3 months)	28	37	0	10	92	11	9	89	13
Iron overload (6 months)	26	41	0	16	95	9	14	95	16

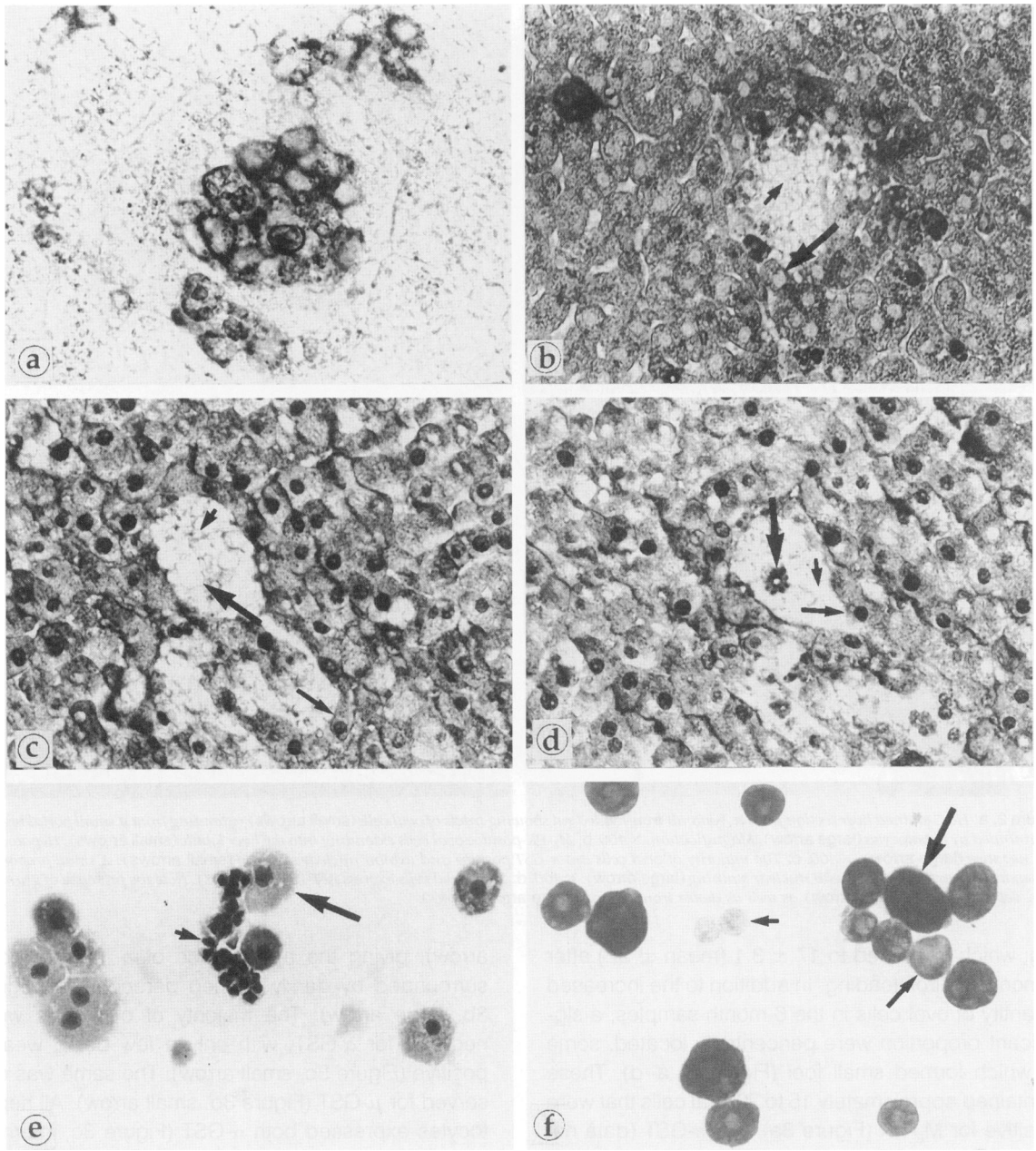

Figure 3. a *to* d: *Liver sections from a 6-month iron-loaded rat showing a small focus of oval cells surrounded by liver parenchyma.* a: *Cluster of* M_2*-PK-positive oval cells. Magnification,* ×*980.* b: *TF-negative focus of oval cells* (small arrow) *among strongly positive hepatocytes* (large arrow). ×*400.* c: *The majority of oval cells are negative for* α*-GST, with only a few being weakly positive* (small arrow). *In contrast, all hepatocytes are strongly positive* (intermediate arrow). *A ductal structure at the center of the focus is negative for* α*-GST* (large arrow). ×*400.* d: *The majority of oval cells are also negative for* μ*-GST* (small arrow) *whereas all hepatocytes are positive* (intermediate arrow). *The same ductal structure shown in* c *strongly expresses* μ*-GST* (large arrow). ×*400.* e: *Liver cells isolated by centrifugal elutriation from rats overloaded with iron for 6 months; H&C stain of fraction 5, containing aggregates of oval cells* (small arrow) *as well as individual hepatocytes* (large arrow). ×*490.* f: *TF-negative isolated oval cells* (small arrow) *shown among a population of heterogeneously stained hepatocytes, some weakly positive* (intermediate arrow) *and some strongly positive* (large arrow). ×*490.*

(Figure 3d, large arrow). Serial sections revealed that the ductal structures did not express α-GST (Figure 3c, large arrow).

There was no evidence of fibrosis or cirrhosis in either the 3- or 6-month iron-loaded liver samples, with no clear evidence of hepatocytic necrosis.

Isolated Cells and Their Pattern of Staining

Cells isolated by centrifugal elutriation allowed more detailed examination and easier quantification of relative numbers that expressed particular markers. Fraction 3 contained mainly oval cells devoid of

hepatocytes, whereas fraction 5 contained aggregates of oval cells (Figure 3e, small arrow) and hepatocytes (Figure 3e, large arrow), allowing comparisons of both cell types to be made on the one slide. For both CDE and iron overload samples, the pattern of immunocytochemical staining obtained from isolated cells correlated well with *in situ* samples.

A summary of the immunocytochemical data from CDE-derived and iron-overload-derived isolated oval cells is presented in Table 1. Greater than 92 and 89% of both CDE- and iron-overload-derived oval cells were positive for M_2-PK and π-GST, respectively. The percentage of oval cells positive for each marker from the 3- and 6-month iron-loaded samples were approximately the same. For the majority of markers, the proportion of positive oval cells obtained by iron overload closely resembled those induced by the CDE diet, with the exception of μ-GST and TF. No more than 14% of iron-derived oval cells expressed μ-GST compared with 28% of CDE-derived oval cells. Similarly, 40% of CDE-derived oval cells expressed TF, whereas none of the oval cells isolated from iron-loaded liver expressed TF (Figure 3f, small arrow). Nearly double the proportion of CDE-derived oval cells expressed L-PK compared with 3-month iron-derived oval cells; however, by 6 months, the proportion of positive iron-derived oval cells (data not shown) was closer to that seen in the CDE group.

Thirty-one percent of hepatocytes isolated from 6-month iron-loaded liver expressed AFP (data not shown), which was not observed in the control liver. The hepatocyte population also exhibited a heterogeneous pattern of L-PK expression (data not shown) and TF expression (Figure 3f, intermediate and large arrows).

Discussion

In models of experimental hepatocarcinogenesis, there are characteristic changes within the liver that precede the development of hepatoma. These changes include the emergence and rapid proliferation of a cellular compartment composed of oval cells. These cells have the ability to generate hepatoma[8] and signify a preneoplastic change in the liver. The present study was undertaken to ascertain whether similar cellular changes occur in iron-overloaded liver.

Numerous studies in experimental iron overload have utilized the rat model.[19,22,23,31,39,43–49] These involved feeding of either carbonyl iron or iron dextran or the intravenous injection of iron. In each instance, iron loading of the liver was a common feature.

The predominantly parenchymal deposition of iron with a periportal distribution observed in the present study agrees with the findings of other researchers.[47] High levels of iron deposition in periportal hepatocytes with a reduction toward pericentral hepatocytes is a clinical feature of genetic hemochromatosis[14,15,22] and indicates the suitability of the carbonyl-iron-fed rat model for studying this disease. We have previously demonstrated the advantages of using π-GST[11] and, more recently, M_2-PK[13] to identify oval cells and apply these to this model. Other markers used were ALB, TF, L-PK, α-GST, μ-GST, and TAT to further compare oval cells obtained from the iron-treated liver with those derived from CDE-treated liver. The majority of oval cells generated from CDE-treated liver expressed M_2-PK and π-GST, with approximately one-third expressing AFP, a similar pattern was found in oval cells derived from iron-overloaded liver. Furthermore, similar proportions of CDE- and iron-derived oval cells expressed ALB, L-PK, α-GST, and TAT. These results indicate that chronic damage induced by iron overload of the liver induces the proliferation of oval cells that are immunocytochemically and morphologically similar to those derived from the liver after administration of the carcinogenic CDE diet, with one exception. Oval cells induced by the iron-loaded diet were TF negative, whereas a substantial proportion of oval cells derived from CDE-treated liver were TF positive. As TF is a transport protein for ferric iron, it is possible that the absence of TF expression is a response to the overabundant levels of iron in the body. Bonkovsky[18] has suggested that iron in hepatocytes stimulates translation of ferritin mRNA and represses transcription of DNA for transferrin and the transferrin receptor. It is possible that a similar process occurs in oval cells. Baynes et al,[50] on the other hand, have reported no evidence of generalized dysregulation of expression of the transferrin receptor in hemochromatosis or in the African form of iron overload. However, the present study supports the idea that iron overload influences the state of hepatocyte TF regulation, as there was an inverse relationship between iron loading and TF expression in hepatocytes.

The significance of the reduced proportion of oval cells expressing μ-GST in the iron group compared with the CDE group is not clear and may reflect a difference in developmental maturity of the two populations of oval cells.

The identification of ductal structures in the iron-loaded liver demonstrates another similarity between CDE-treated and iron-loaded liver. Ductal structures, thought to be derived from oval cells, are distinct from normal bile ducts in several respects. Bile ducts reside in the portal triad whereas ductal structures are randomly located throughout the liver lobule after extensive oval cell proliferation. Furthermore, these structures are absent in normal liver and express different markers to normal bile duct cells. In a previous study,[11] we demonstrated that CDE-derived duct-like structures expressed α- and π-GST but not μ-GST, which is expressed by normal bile ducts. In contrast, the ductal structures identified in this study expressed μ-GST, suggesting a closer association to normal bile duct cells than the duct-like structures evident in CDE-treated liver.

It has been reported that human liver biopsies from GH patients vary greatly with respect to histological findings, ranging from normal to those displaying micronodular cirrhosis.[15] Therefore, the absence of fibrotic or cirrhotic change in this study is not surprising, especially when it is normally associated with more advanced stages of GH.

We have previously reported the expression of AFP in the hepatocyte population during the early stages of experimental hepatocarcinogenesis as well as in ethanol-treated liver.[13] The expression of AFP in a proportion of iron-loaded hepatocytes may be a response to chronic damage and possibly indicates an early stage of preneoplasia.

In cirrhotic patients, regenerating nodules have occasionally exhibited smaller amounts of excess iron than the rest of the liver.[15] Liver biopsies from patients with GH complicated with hepatocellular carcinoma, contain iron-free foci,[30] shown to be proliferative lesions, strongly suggesting that they are preneoplastic.[24,30,51] Future studies may reveal a relationship between these preneoplastic iron-free foci and the iron-free oval cells reported in this study.

References

1. Sell S, Leffert HL: An evaluation of cellular lineages in the pathogenesis of experimental hepatocellular carcinoma. Hepatology 1982, 2:77–86
2. Farber E: Similarities in the sequence of early histological changes induced in the liver of the rat by ethionine, 2-acetylaminofluorene, and 3′-methyl-4-dimethylaminoazobenzene. Cancer Res 1956, 16:142–148
3. Hayner NT, Braun L, Yaswen P, Brooks M, Fausto N: Isozyme profiles of oval cells, parenchymal cells, and biliary cells isolated by centrifugal elutriation from normal and preneoplastic livers. Cancer Res 1984, 44: 332–328
4. Dunsford HA, Maset R, Salman J, Sell S: Connection of ductlike structures induced by a chemical hepatocarcinogen to portal bile ducts in the rat liver detected by injection of bile ducts with a pigmented barium gelatin medium. Am J Pathol 1985, 118:218–224
5. Evarts RP, Nagy P, Marsden E, Thorgeirsson SS: *In situ* hybridization studies on expression of albumin and α-fetoprotein during the early stage of neoplastic transformation in rat liver. Cancer Res 1987, 47:5469–5475
6. Germain L, Noel M, Gourdeau H, Marceau N: Promotion of growth and differentiation of rat ductular oval cells in primary culture. Cancer Res 1988, 48:368–378
7. Evarts RP, Nagy P, Nakatsukasa H, Marsden E, Thorgeirsson SS: *In vivo* differentiation of rat liver oval cells into hepatocytes. Cancer Res 1989, 49:1541–1547
8. Braun L, Mikumo R, Fausto N: Production of hepatocellular carcinoma by oval cells: cell cycle expression of c-*myc* and p53 at different stages of oval cell transformation. Cancer Res 1989, 49:1554–1561
9. Praet M, Roels H, van Oostveldt P: Early liver cell lesions in rats induced by thioacetamide: an ultrastructural, cytophotometric and autoradiographic study. Pathol Res Pract 1989, 184:69–76
10. Yaswen P, Hayner NT, Fausto N: Isolation of oval cells by centrifugal elutriation and comparison with other cell types purified from normal and preneoplastic livers. Cancer Res 1984, 44:324–331
11. Tee LB, Smith PG, Yeoh GC: Expression of α, μ, and π class glutathione S-transferases in oval and ductal cells in liver of rats placed on a choline-deficient, ethionine-supplemented diet. Carcinogenesis 1992, 13: 1879–1885
12. Hsia CC, Evarts RP, Nakatsukasa H, Marsden ER, Thorgeirsson SS: Occurrence of oval-type cells in hepatitis B virus-associated human hepatocarcinogenesis. Hepatology 1992, 16:1327–1333
13. Smith PGJ, Tee LBG, Yeoh GCT: Appearance of oval cells in the liver of rats chronically exposed to ethanol. Hepatology 1996, 23:145
14. Bacon BR: Causes of iron overload. N Engl J Med 1992, 326:126–127
15. Bacon BR, Britton RS: The pathology of hepatic iron overload: a free radical-mediated process? Hepatology 1990, 11:127–137
16. Stremmel W, Riedel HD, Niederau C, Strohmeyer G: Pathogenesis of genetic haemochromatosis. Eur J Clin Invest 1993, 23:321–329
17. Chapman DE, Good MF, Powell LW, Halliday JW: The effect of iron, iron-binding proteins, and iron-overload on human natural killer cell activity. J Gastroenterol Hepatol 1988, 3:9–17
18. Bonkovsky HL: Iron and the liver. Am J Med Sci 1991, 301:32–43
19. Bacon BR, O'Neill R, Britton RS: Hepatic mitochondrial

energy production in rats with chronic iron overload. Gastroenterology 1993, 105:1134–1140
20. Kew MD: Pathogenesis of hepatocellular carcinoma in hereditary hemochromatosis: occurrence in noncirrhotic patients. Hepatology 1990, 11:1086–1087
21. Brown EB: Iron metabolism: a 40-year overview. Am J Med 1989, 87:35–39
22. Bacon BR, Tavill AS, Brittenham GM, Park CH, Recknagel RO: Hepatic lipid peroxidation *in vivo* in rats with chronic iron overload. J Clin Invest 1983, 71:429–439
23. Bacon BR, Park CH, Brittenham GM, O'Neill R, Tavill AS: Hepatic mitochondrial oxidative metabolism in rats with chronic dietary iron overload. Hepatology 1985, 5:789–797
24. Deugnier YM, Guyader D, Crantock L, Lopez JM, Turlin B, Yaouang J, Jouanolle H, Campion JP, Launois B, Halliday JW, et al: Primary liver cancer in genetic hemochromatosis: a clinical, pathological, and pathogenetic study of 54 cases. Gastroenterology 1993, 104:228–234
25. Fargion S, Mandelli C, Piperno A, Cesana B, Fracanzani AL, Fraquelli M, Bianchi PA, Fiorelli G, Conte D: Survival and prognostic factors in 212 Italian patients with genetic hemochromatosis. Hepatology 1992, 15: 655–659
26. Fargion S, Piperno A, Fracanzani AL, Cappellini MD, Romano R, Fiorelli G: Iron in the pathogenesis of hepatocellular carcinoma. Ital J Gastroenterol 1991, 23: 584–588
27. Borecki IB, Rao DC, Le Mignon L, Yaouang J, Simon M, Lalouel JM: Genetic hemochromatosis: distribution analysis of six laboratory measures of iron metabolism. Am J Med Genet 1989, 34:435–441
28. Hauser SC: Hemochromatosis and the heart. Heart Dis Stroke 1993, 2:487–491
29. Neiderau C, Fischer R, Sonnenberg A, Stremmel W, Trampisch HJ, Strohmeyer G: Survival and causes of death in cirrhotic and in noncirrhotic patients with primary hemochromatosis. N Engl J Med 1985, 313: 1256–1262
30. Deugnier YM, Charalambous P, Le Quilleuc D, Turlin B, Searle J, Brissot P, Powell LW, Halliday JW: Preneoplastic significance of hepatic iron-free foci in genetic hemochromatosis: a study of 185 patients. Hepatology 1993, 18:1363–1369
31. Britton RS, Ferrali M, Magiera CJ, Recknagel RO, Bacon BR: Increased prooxidant action of hepatic cytosolic low-molecular-weight iron in experimental iron overload. Hepatology 1990, 11:1038–1043
32. Sharma BK, Bacon BR, Britton RS, Park CH, Magiera CJ, O'Neill R, Dalton N, Smanik P, Speroff T: Prevention of hepatocyte injury and lipid peroxidation by iron chelators and α-tocopherol in isolated iron-loaded rat hepatocytes. Hepatology 1990, 12:31–39
33. von Herbay A, de Groot H, Hegi U, Stremmel W, Strohmeyer G, Sies H: Low vitamin E content in plasma of patients with alcoholic liver disease, hemochromatosis, and Wilson's disease. J Hepatol 1994, 20:41–46
34. Loreal O, Deugnier Y, Moirand R, Lauvin L, Guyader D, Jouanolle H, Turlin B, Lescoat G, Brissot P: Liver fibrosis in genetic hemochromatosis: respective roles of iron and non-iron-related factors in 127 homozygous patients. J Hepatol 1992, 16:122–127
35. Thorstensen K, Romslo I: The role of transferrin in the mechanism of cellular iron uptake. Biochem J 1990, 271:97–105
36. Bacon BR, Fried MW, DiBisceglie AM: A 39-year-old man with chronic hepatitis, elevated serum ferritin values, and a family history of hemochromatosis. Semin Liver Dis 1993, 13:101–105
37. Deugnier Y, Battistelli D, Jouanolle H, Guyader D, Gueguen M, Loreal O, Jacquelinet C, Bourel M, Brissot P: Hepatitis B virus infection markers in genetic haemochromatosis: a study of 272 patients. J Hepatol 1991, 13:286–90
38. Di Bisceglie AM, Axiotis CA, Hoofnagle JH, Bacon BR: Measurements of iron status in patients with chronic hepatitis. Gastroenterology 1992, 102:2108–2113
39. Irving MG, Booth CJ, Devlin CM, Halliday JW, Powell LW: The effect of iron and ethanol on rat hepatocyte collagen synthesis. Comp Biochem Physiol C 1991, 100:583–590
40. Palazzo JP, Lundquist K, Mitchell D, Mittal KR, Hann HW, Munoz S, Moritz MJ, Jacobs JM, Martin P: Rapid development of lymphoma following liver transplantation in a recipient with hepatitis B and primary hemochromatosis. Am J Gastroenterol 1993, 88: 102–104
41. Piperno A, Fargion S, D'Alba R, Roffi L, Fracanzani AL, Vecchi L, Failla M, Fiorelli G: Liver damage in Italian patients with hereditary hemochromatosis is highly influenced by hepatitis B and C virus infection. J Hepatol 1992, 16:364–368
42. Seglen PO: Preparation of rat liver cells. I. Effect of Ca^{2+} on enzymatic dispersion of isolated, perfused liver. Exp Cell Res 1972, 74:450–454
43. Adams PC, Chau LA: Hepatic ferritin uptake and hepatic iron. Hepatology 1990, 11:805–808
44. Andrews SC, Brady MC, Treffry A, Williams JM, Mann S, Cleton MI, de Bruijn W, Harrison PM: Studies on haemosiderin and ferritin from iron-loaded rat liver. Biol Metals 1988, 1:33–42
45. Britton RS, O'Neill R, Bacon BR: Chronic dietary iron overload in rats results in impaired calcium sequestration by hepatic mitochondria and microsomes [published erratum appears in Gastroenterol 1991, 101: 1761]. Gastroenterology 1991, 101:806–811
46. Britton RS, O'Neill R, Bacon BR: Hepatic mitochondrial malondialdehyde metabolism in rats with chronic iron overload. Hepatology 1990, 11:93–97
47. Roberts FD, Charalambous P, Fletcher L, Powell LW, Halliday JW: Effect of chronic iron overload on procollagen gene expression. Hepatology 1993, 18:590–595
48. Figueiredo MS, Baffa O, Barbieri Neto J, Zago MA:

Liver injury and generation of hydroxyl free radicals in experimental secondary hemochromatosis. Res Exp Med (Berl) 1993, 193:27–37

49. Levy P, Dumont M, Brissot P, Letreut A, Favier A, Deugnier Y, Erlinger S: Acute infusions of bile salts increase biliary excretion of iron in iron-loaded rats. Gastroenterology 1991, 101:1673–1679
50. Baynes RD, Cook JD, Bothwell TH, Friedman BM, Meyer TE: Serum transferrin receptor in hereditary hemochromatosis and African siderosis. Am J Hematol 1994, 45:288–292
51. Deugnier YM, Loreal O, Turlin B, Guyader D, Jouanolle H, Moirand R, Jacquelinet C, Brissot P: Liver pathology in genetic hemochromatosis: a review of 135 homozygous cases and their bioclinical correlations. Gastroenterology 1992, 102:2050–2059